Ankle loading ameliorates bone loss from breast cancer–associated bone metastasis

Shuang Yang,[*,†] Hong Liu,[‡,§,¶,‖] Lei Zhu,[§,#] Xinle Li,[*,†] Daquan Liu,[*,†] Xiaomeng Song,[*] Hiroki Yokota,[**] and Ping Zhang[*,†,**,††,1]

*Department of Anatomy and Histology, School of Basic Medical Sciences, †Key Laboratory of Hormones and Development, Ministry of Health, Tianjin Key Laboratory of Metabolic Diseases, ‖Key Laboratory of Cancer Prevention and Therapy, Ministry of Education, and ††Tianjin Key Laboratory of Spine and Spinal Cord, Tianjin Medical University, Tianjin, China; ‡Department of Breast Surgery and #Department of Molecular Imaging and Nuclear Medicine, National Clinical Research Center for Cancer, Tianjin Medical University Cancer Institute and Hospital, Tianjin, China; §Key Laboratory of Cancer Prevention and Therapy, Tianjin, China; ¶Tianjin's Clinical Research Center for Cancer, Tianjin, China; and **Department of Biomedical Engineering, Indiana University–Purdue University Indianapolis, Indianapolis, Indiana, USA

ABSTRACT: Breast cancer is a serious health problem that preferentially metastasizes to bone. We have previously shown that bone loss can be prevented by mechanical loading, but the efficacy of ankle loading for metastasis-linked bone loss has not been investigated. This study showed that body weight was decreased after inoculation of tumor cells, but ankle loading restored a rapid weight loss. The nonloading group exhibited a decrease in bone volume/tissue volume (BV/TV), trabecular thickness, and trabecular number (all $P < 0.01$) as well as an increase in trabecular separation ($P < 0.001$). However, ankle loading improved those changes (all $P < 0.05$). Furthermore, although the nonloading group increased the tumor bearing as well as expression of IL-8 and matrix metalloproteinase 9, ankle loading decreased them. Induction of tumor in the bone elevated the osteoclast number ($P < 0.05$) as well as the levels of nuclear factor of activated T-cells cytoplasmic 1, NF-κB ligand, cathepsin K, and serum tartrate-resistant acid phosphatase type 5b, but ankle loading reduced osteoclast activity and those levels (all $P < 0.05$). Tumor bearing was positively correlated with the osteoclast number ($P < 0.01$) and negatively correlated with BV/TV and the osteoblast number (both $P < 0.01$). Collectively, these findings demonstrate that ankle loading suppresses tumor growth and osteolysis by inhibiting bone resorption and enhancing bone formation.—Yang, S., Liu, H., Zhu, L., Li, X., Liu, D., Song, X., Yokota, H., Zhang, P. Ankle loading ameliorates bone loss from breast cancer–associated bone metastasis. FASEB J. 33, 000–000 (2019). www.fasebj.org

KEY WORDS: mechanical loading · tumor · osteolysis · osteoclast · osteoblast

Breast cancer is the most common cancer among women in the world (1), and in China, recent incidence of breast cancer has continued to rise 3% annually (2). Eighty percent of patients with breast cancer in the advanced stage suffer from bone metastasis (3, 4). Bone metastases from breast cancer are usually associated with refractory bone pain and pathologic fractures. Although proven strategies of clinical treatment include surgery, radiotherapy, endocrine therapy, chemotherapy, and targeted therapies (5, 6), no significant effect on survival or patient quality of life is clearly observed (7–9).

Epidemiologic reports indicate that physical activity reduces the risk of inducing a variety of cancers. It is commonly considered that physical activity also improves the sequelae during cancer treatment. Multiple meta-analyses reveal that physical activity reduces incidence of mortality of breast cancer, and it improves quality of life (10–13). Many lines of evidence also suggest that it is capable of decelerating a decline in physical performance (14). For instance, voluntary wheel running decreases incidence and progression of tumors, including skin, liver, and lung cancers in preclinical studies (15). Collectively, physical activity could be a unique form of adjutant therapies for patients with breast cancer and bone metastases (16). There are varying types of mechanical loading, which, in part, mimics physical activity. Although low-intensity vibration and *in vivo* tibial compression are reported to inhibit bone loss from metastatic tumors, the

potential role of ankle loading as an anti-tumor agent has not been investigated in any previous studies (17, 18). Ankle loading is a form of joint loading, similar to knee loading and elbow loading, which has been shown to induce both local and systemic loading effects.

Bone histomorphometric studies demonstrate that joint loading stimulates bone formation, accelerates fracture healing, and improves bone strength (19–21). Our previous studies also reveal that joint loading reduces skeletal inflammation and degradation, and it may offer a novel physical regimen for osteoarthritis and osteonecrosis (22, 23). Ankle loading, 1 form of joint loading, is an effective means to induce bone formation throughout periosteal and endosteal diaphysis of the tibia by activating signaling pathways, such as PI3K, extracellular matrix–receptor interactions, TGF-β signaling, and Wnt signaling (19–21). This study was focused on the effects of ankle loading on bone homeostasis in the presence of mammary tumor cells in the tibia. In breast cancer–associated bone metastasis, the distal tibia, a loading site with ankle loading, is not a primary target of breast cancer–associated metastasis (24). Thus, any benefit from ankle loading is considered to be related to its indirect loading effects, including the possibility of bone protection at a tumor-driven pathogenic site in the proximal tibia.

Although bone structure is controlled in part by a balance between bone-resorbing osteoclasts and bone-forming osteoblasts, the majority of breast cancer–associated bone metastases lead to osteolytic lesion, but there is also osteoblast bone lesion. Tumors stimulate differentiation and maturation of osteoclasts, leading to bone resorption and bone loss. The bone matrix also releases a variety of pro-tumorigenic growth factors that lead to a vicious cycle (25). IL-8 has pleiotropic effects on cancer cells and can impact many stages of tumor progression. IL-8 also has potent pro-osteoclastogenic activity and is identified as an osteolytic factor. Its overexpression in breast cancer has been observed, and its elevated serum level is associated with osteolysis and bone metastasis (26, 27). The invasive role of matrix metalloproteinases (MMPs) has been known in many types of cancers, including breast cancer. MMP9 has been linked to proliferation and invasion of breast cancer cells. It is reported that flow-stimulated osteocytes down-regulate the bone-metastatic potential of breast cancer cells and that breast cancer cell expression of MMP9 was down-regulated (28, 29). We addressed the question of whether ankle loading, indirect loading separated away from the site of tumor growth in bone, would be beneficial for protecting bone from breast cancer–associated metastases.

In this study, we hypothesized that ankle loading suppresses tumor growth and osteolysis by inhibiting bone resorption and enhancing bone formation. To test the hypothesis, we employed a mouse model of breast cancer–associated bone metastases in which tumor cells were intratibially injected to induce tumor growth in the tibia. The ankle joint received loads at 5 Hz for 5 min/d for 3 wk. In evaluation of ankle loading, we focused on bone microstructure, tumor bearing, bone resorption and formation using X-ray imaging, microcomputed tomographic (micro CT) imaging, and histologic analysis. The correlational relationship among bone volume/tissue volume (BV/TV), osteoclast number, osteoblast number, and tumor burden, as well as among IL-8, MMP9, nuclear factor of activated T-cells cytoplasmic 1 (NFATc1), and serum tartrate-resistant acid phosphatase type 5b (TRACP-5b) was examined. To determine the mechanism of ankle loading action, we evaluated the role of specific molecular mediators that are linked to osteolysis and bone metastases.

MATERIALS AND METHODS

Animals and material preparation

BALB/c female mice (~6 wk of age, Animal Center of Academy of Military Medical Sciences, Beijing, China) were maintained, with 5 animals per cage, in a 12-h light/dark cycle condition with access to food and water *ad libitum*. All experiments were executed based on the *Guide for Care and Use of Laboratory Animals* (National Institutes of Health, Bethesda, MD, USA) and were approved by the Ethics Committee of Tianjin Medical University. The mouse mammary tumor cell line, 4T1, was obtained from American Type Culture Collection (Manassas, VA, USA). Roswell Park Memorial Institute 1640 basic medium, fetal bovine serum, penicillin/streptomycin, nonessential amino acid, and 0.25% trypsin were purchased from Thermo Fisher Scientific (Waltham, MA, USA). An ELISA kit for TRACP-5b was purchased from Immunodiagnostics System (Scottsdale, AZ, USA). An immunohistochemical staining kit and a 3, 3'-diaminobenzidine substrate kit were purchased from ZSGB Biotechnology (Beijing, China). Antibodies for NFATc1, IL-8, MMP9, and β-actin were obtained from Abcam (Cambridge, MA, USA), and for NF-κB ligand (RANKL) were purchased from PeproTech (Rocky Hill, NJ, USA), and antibody for cathepsin K was acquired from Proteintech Group (Rosemont, IL, USA). Other chemicals were purchased from MilliporeSigma (Burlington, MA, USA).

Experimental design

Forty-five mice were randomly divided into 3 groups: a nontumor group (sham–no tumor), a tumor group with tumor injection (nonloading), and a loading group with tumor injection (loading) (n = 15). Tumor in bone was induced by intratibial injection of 4T1 cells using the procedure previously described (30). Body weights were recorded every 5 d for monitoring an overall health condition (**Fig. 1***A*).

Body weight and analysis of body fat composition

The body weight and food intake of each mouse were measured weekly and daily, respectively, by a person blinded to each group. Lean mass and fat mass were measured every week by peripheral dual-energy X-ray absorptiometry.

Animal model of intratibia injection

4T1 cells were maintained in complete 1640 medium with the addition of 10% fetal bovine serum, 1% penicillin/streptomycin, and 1% nonessential amino acid. The cells were incubated in a 37°C and 5% CO_2 incubator according to the standard protocol.

The 4T1 cells were injected into the right tibia as previously described (30). Briefly, mice were sedated in an isolation
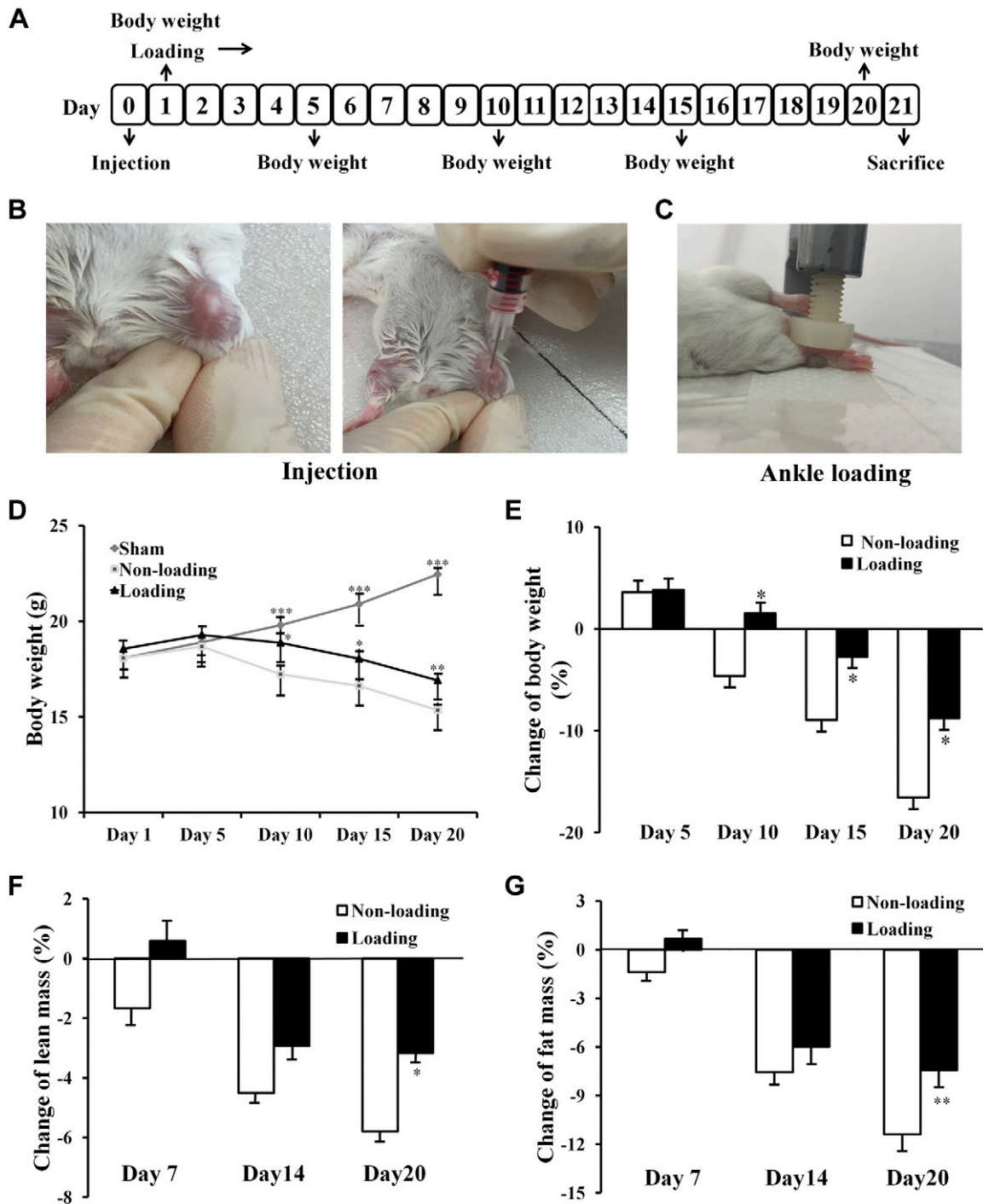
Figure 1. The effect of loading on body weight and body composition with 4T1 cell injection. *A*) Timeline of the study. *B*) Intratibial injection in the proximal tibia. *C*) Lateral loading applied to the right ankle (1 N at 5 Hz for 5 min/d) for 3 wk. *D*) Mean body weight on d 1, 5, 10, 15, and 20. *E*) Changes in body weight. *F*) Changes in body lean mass. *G*) Changes in body fat mass. *P < 0.05, **P < 0.01, and ***P < 0.001 (n = 10).

chamber, and mask-anesthetized using 1.5% isoflurane (Iso-Flo; Abbott Laboratories, Lake Bluff, IL, USA) at a flow rate of 0.6–1 L/min. An animal was placed on its back with chest facing up, and a knee joint was exposed and cleaned with 70% ethanol. With the knee in the bent state, the cell suspension (1×10^4 cells suspended in 25 µl sterile PBS) was injected in the underlying patella through the middle of the patellar ligament and into the medullary cavity of the proximal tibia (Fig. 1B) using a 29-gauge disposable insulin syringe. Using

the same procedure, 25 µl PBS was injected in the right tibia of the sham-treated group.

Ankle loading

One day after tumor injection, ankle loading was initiated using pulsed loads to the right ankle joint in the lateral-medial direction as previously described (Fig. 1C) (19). The loading was given for

3 wk with 1 N force at 5 Hz for 5 min/d. Mice in the sham-treated control group and nonloading model group were placed on the loading device without applying any dynamic loads. During loading, a mouse was maintained under inhalation of anesthesia using 1–1.5% isoflurane at a flow rate of 0.6–1 L/min. Mice were euthanized 3 wk after onset of ankle loading. Tibias were separated from soft tissue and fixed in 10% neutral formaldehyde solution for 48 h.

X-ray imaging

Osteolytic lesion area and abnormal bone remodeling can be visualized and assessed *in vivo* using an X-ray machine. The mice were sedated, anesthetized, and subjected to digital X-ray imaging of the middle region of the hind limbs using a Kodak *In Vivo* Imaging Systems (Carestream Health, Rochester, NY, USA). All images were acquired using the following parameters: 60,000 s exposure time; 2×2 binning; 60 s acquisition time; 120×120-mm field of view; and f 2.25 aperture stop (30).

Microcomputed tomography

To determine 3-dimensional architecture, the tibiae were scanned using micro CT. Formalin-fixed tibias were scanned by a micro CT 40 (Viva CT 40; Scanco Medical, Wangen-Brüttisellen, Switzerland). The selected parameters for scanning were 70 kV, 110 μA, 0.5-mm aluminum filter, 1k camera resolution, 10.5-μm voxel size, 0.5° rotation step, and 180° tomographic rotation. The regions of interest were distal to the growth plate with 250 cross-sectional slices. Three-dimensional images were reconstructed from CT slices, and 2- and 3-dimensional morphometric parameters were determined. Measurements included tibial integrity (%, number of intact tibias/total number of tibias; number of degraded tibias/total number of tibias), fractional bone volume (BV/TV), trabecular thickness (Tb.Th; mm), trabecular number (Tb.N; mm^{-1}), and trabecular separation (Tb.Sp; mm) (17).

Histology and immunohistochemistry assay

Tibia samples were decalcified by EDTA (14% EDTA, pH 7.3) for 20 d and embedded in paraffin. The specimens were cut into consecutive, longitudinal, 5-μm-thick sections. Pathology slices were deparaffinized in xylene and rehydrated in an ethanol gradient for hematoxylin and eosin (H&E) staining, tartrate-resistant acid phosphatase (TRAP) staining, and MacNeal's staining. Images of complete histologic sections were captured and evaluated using Image-Pro software (Media Cybernetics, Rockville, MD, USA).

H&E staining was used to evaluate tumor burden, tumor area/total tissue area (TuAr/Tar; in %). One of every 10 slices, a total of 3 slices, were chosen for quantification in each tissue. The slices were counted at ×40 magnification using the sections distal to the proximal growth plate in the tibia (17, 31). TRAP staining was conducted for evaluating osteoclast activation (32, 33). The ratio between lengths of TRAP-positive cells and total circumference of bone trabecula [osteoclast surface (Oc.S)/bone surface (BS), %] was calculated. MacNeal's staining was used to determine osteoblast activity and osteoblast number by the trabecular bone surface (N. Ob/BS, osteoblast number/bone surface, mm) was calculated (34).

The expressions of NFATc1, IL-8, and MMP9 were analyzed by immunohistochemistry. After deparaffination and rehydration, antibodies were used at a 1:50 dilution overnight at 4°C. An immunohistochemical color reaction was performed using a 3, 3'-diaminobenzidine substrate kit. Slides were counterstained

with hematoxylin and dehydrated. The number of positively stained cells was counted in the area per specimen, and 5 sequential specimens per mouse were measured in each group in a blinded fashion.

ELISA assay

The TRACP-5b, a bone resorption marker of bone turnover markers, was used as a marker for osteoclasts (35, 36). The serum was collected when animals were euthanized and was stored at −80°C. The serum was thawed for detecting TRACP-5b using an ELISA kit according to the manufacturer's instructions.

Western blot assay

Bone tissues were powdered and lysed in a RIPA lysis buffer, which contained the inhibitors of proteases and phosphatases (Roche, Basel, Switzerland). The levels of cathepsin K, RANKL, and β-actin were determined by Western blotting. The samples were size-fractionated in a sodium dodecyl sulfate-polyacrylamide gel and transferred onto the PVDF membrane. The membranes with primary antibodies were incubated overnight at 4°C (cathepsin K 1:2000, RANKL 1:4000, and β-actin 1:10,000). The membranes were then washed and incubated with horseradish peroxidase–conjugated secondary antibody (1:20,000). ECL was used to assess protein expression, image acquisition, and analysis software (Bio-Rad, Hercules, CA, USA) was used to quantify and intensities.

Statistical analysis

Data were expressed as means $\pm$ SD and were analyzed with independent-sample Student's t test (for 2 groups), or 1-way ANOVA (for more than 2 groups). For pair-wise comparisons, a *post hoc* test was conducted using Fisher's protected least significant difference. Correlation analysis of parameters was performed by using Pearson correlation coefficient test. Statistical significance was assumed at $P < 0.05$.

RESULTS

Ankle loading restored body weight loss

Mean body weight and change in body weight were determined on d 1, 5, 10, 15, and 20 (Fig. 1C, D). During a 3-wk period, the nonloading model group with injection of 4T1 cells lost weight at a fastest pace. Compared with the sham-treated group, the nonloading group significantly reduced weight from the first week ($P < 0.001$; Fig. 1D). However, compared with the nonloading group, ankle loading improved weight loss ($P < 0.05$; Fig. 1E). Compared with the nonloading group, ankle loading increased lean mass ($P < 0.05$) and fat mass ($P < 0.01$) from the second week (Fig. 1F, G).

Ankle loading improved osteolysis and cancellous bone microarchitecture

To analyze the effect of ankle loading on bone remodeling, cancellous mass and bone architecture were evaluated
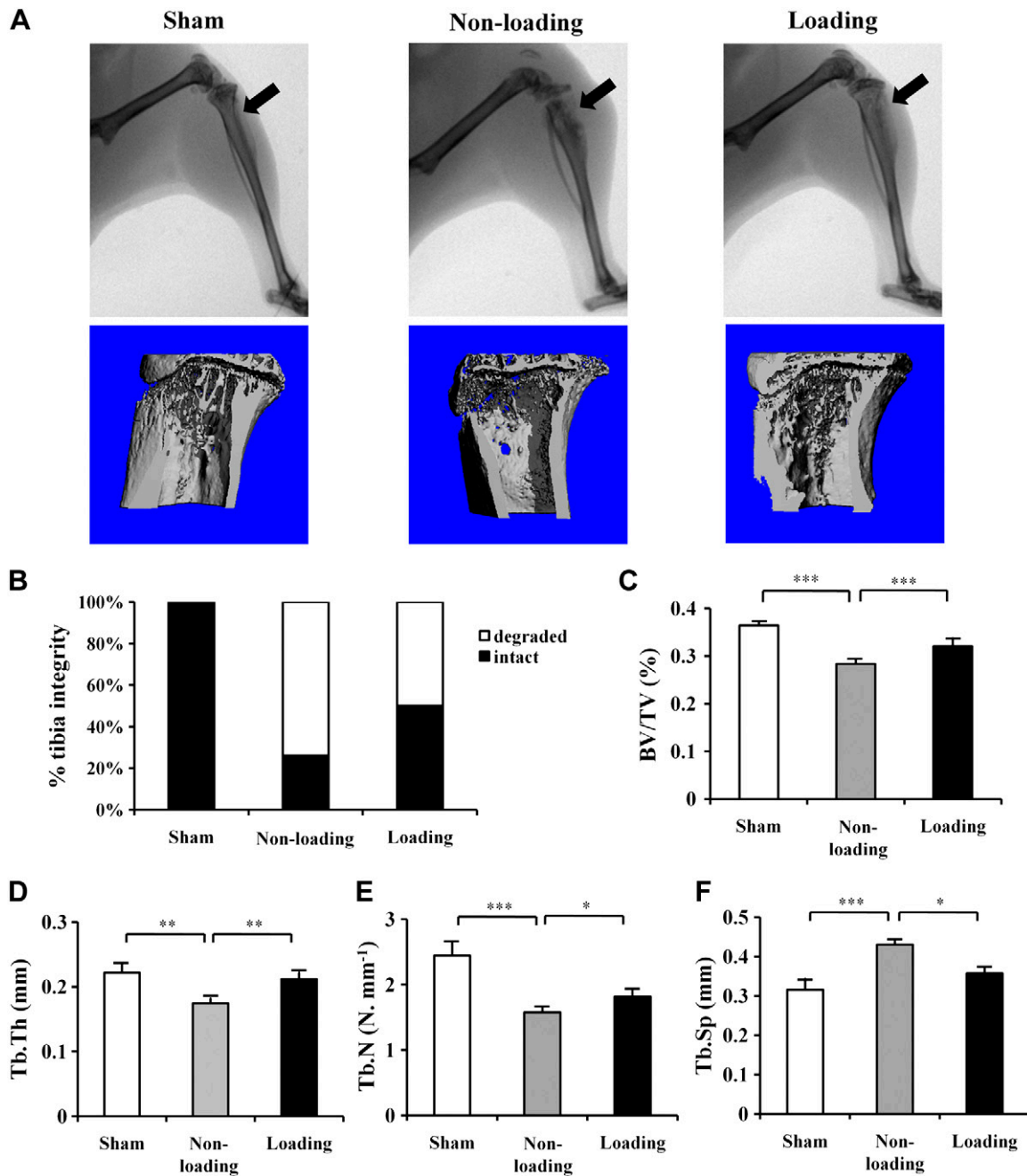
Figure 2. X-ray and micro CT images of the proximal tibia. *A) In vitro* 3-dimensional reconstruction. The representative pictures are presented for the entire length of the tibia and the proximal region of the tibia. *B)* Tibial integrity. *C–F)* Parameters of micro CT imaging. Ankle loading increased fractional bone volume (BV/TV) (*C*), Tb.Th (*D*), and Tb.N (*E*) compared with the nonloading group without loading. Furthermore, ankle loading reduced Tb.Sp (*F*) compared with the nonloading group (*n* = 10). Loading, loading group; nonloading, nonloading group; sham,sham control group. The osteolytic site was indicated by the black arrow. *$P < 0.05$, **$P < 0.01$, and ***$P < 0.001$.

using X-ray and micro CT imaging. Compared with the sham-treated group, tumor cells in the nonloading group caused osteolytic lesions, reduced trabecular bone, generated cavitation of cortical bone, and reduced tibia integrity in the model group (**Fig. 2*A, B***). In contrast, ankle loading markedly suppressed osteolysis and improved bone microarchitecture. Compared with the nonloading model group, the loading group significantly enhanced BV/TV ($P < 0.001$), Tb.Th ($P < 0.01$), and Tb.N ($P < 0.05$), with a decrease in Tb.Sp ($P < 0.05$) (Fig. 2*C–F*).

Ankle loading significantly inhibited tumor growth and metastasis to bone

To examine the effect of ankle loading on cancellous bone, we evaluated the degree of tumor bearing. Histologic examination clearly showed that tumor burden (TuAr/TAr) was significantly reduced with ankle loading ($P < 0.001$; **Fig. 3*A, B***).

To further evaluate the effect of ankle loading, we examined expression of the selected metastasis-related

Figure 3. Reduction of intratibially injected tumor by ankle loading. *A*) Representative images of H&E staining of the tibial sections (original magnification, ×40; scale bar, 500 μm). The TuAr was indicated by the solid line. *B*) Histomorphometric evaluation of the TuAr/Tar ratio. *C, E*) Expression of IL-8 (*C*) and MMP9 (*E*) detected by immunohistochemistry (original magnification, ×400; scale bar, 50 μm). The positive signal is indicated by the arrow. *D, F*) Quantification of IL-8 (*D*) and MMP9 (*F*)-positive cells in the tibia (*n* = 10). ***$P < 0.001$.
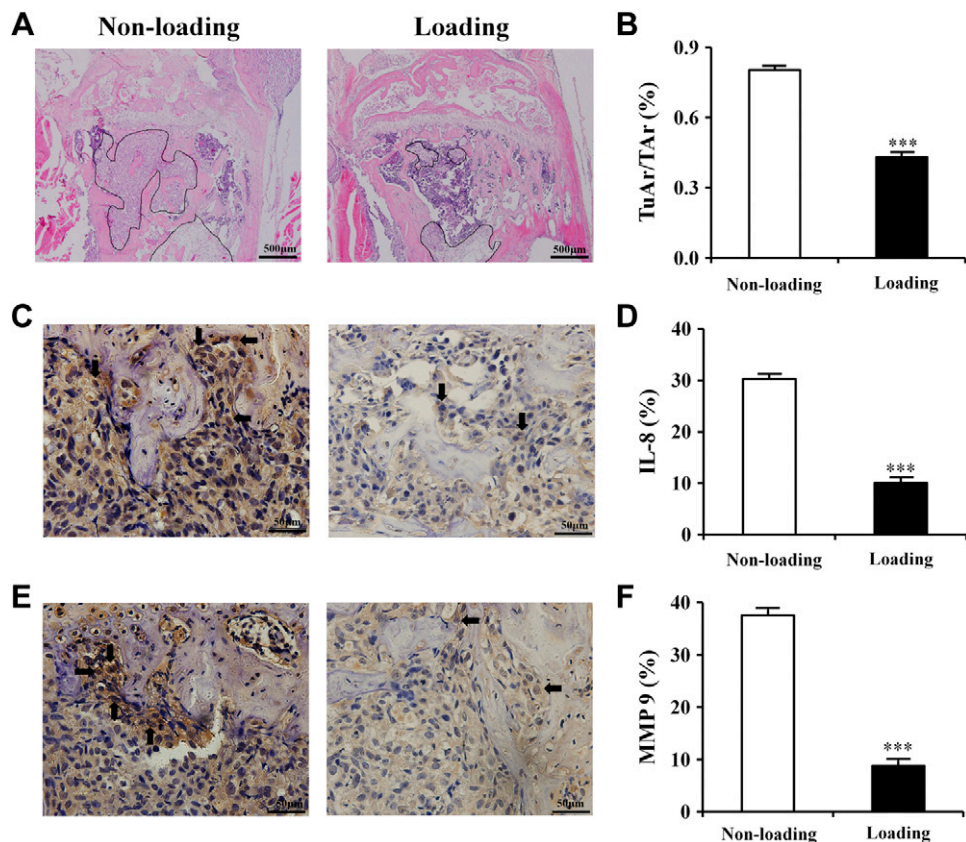
factors, such as IL-8 and MMP9. Immunohistochemical analysis showed that the nonloading model group elevated expression of IL-8 and MMP9, and ankle loading decreased their expression levels (both $P < 0.001$; Fig. 3*C–F*).

Ankle loading significantly suppressed bone resorption

To determine the effect of ankle loading on bone resorption, TRAP staining was conducted (**Fig. 4***A*). The nonloading group showed more TRAP-positive cells that the loading group ($P < 0.05$; Fig. 4*B*). We further examined expression of a transcription factor NFATc1 as well as osteoclast markers. Immunohistochemical analysis revealed that expression of NFATc1 was higher in the nonloading group than in the loading group and ankle loading significantly suppressed bone resorption ($P < 0.05$; Fig. 4*C, D*). Compared with the nonloading group, the loading group also decreased the level of RANKL and cathepsin K (both $P < 0.05$; Fig. 4*E, F*). Compared with the nonloading group, there was a substantial decrease of serum TRACP-5b level in the loading group ($P < 0.01$; Fig. 4*G*).

MacNeal's staining was used to identify osteoblasts that were located on the trabecular surface of the tibia. The result showed that the number of osteoblasts was significantly increased in the loading group ($P < 0.05$; Fig. 4*H, I*).

The correlations between osteoclast, osteoblast, and tumor burden in breast cancer bone metastasis

To evaluate the role of osteoclasts in breast cancer–associated bone metastasis, correlation analysis of tumor burden with BV/TV, osteoclast number, and osteoblast number was conducted. First, the bone fraction (BV/TV) in the tibia was negatively correlated with the TuAr/Tar ratio ($r = -0.947$, $P < 0.01$; **Fig. 5***A*). Second, the number of osteoclast in the tibia was positively correlated with TuAr/Tar ($r = 0.927$, $P < 0.01$; Fig. 5*B*). Third, the number of osteoblasts (N.Ob/BS) was negatively correlated with TuAr/TAr ($r = -0.834$, $P < 0.01$; Fig. 5*C*).

Correlation analysis among IL-8, MMP9, and NFATc1 was also conducted to evaluate any link between tumor metastasis and osteoclasts. Both IL-8 and MMP9 were positively correlated with NFATc1 ($r = 0.780, 0.728$, $P < 0.01$; Fig. 5*D, E*), and the number of osteoclasts (Oc.S/BS) was also positively correlated with IL-8 ($r = 0.775$, $P < 0.01$; Fig. 5*F*).

DISCUSSION

In this preclinical study, we evaluated the possibility of unique physical treatment for preventing bone loss from breast cancer–associated bone metastasis. In the mouse model, tumor and osteolysis were induced by intratibia injection. Although the nonloading group presented quick loss of body weight, ankle loading marginally but
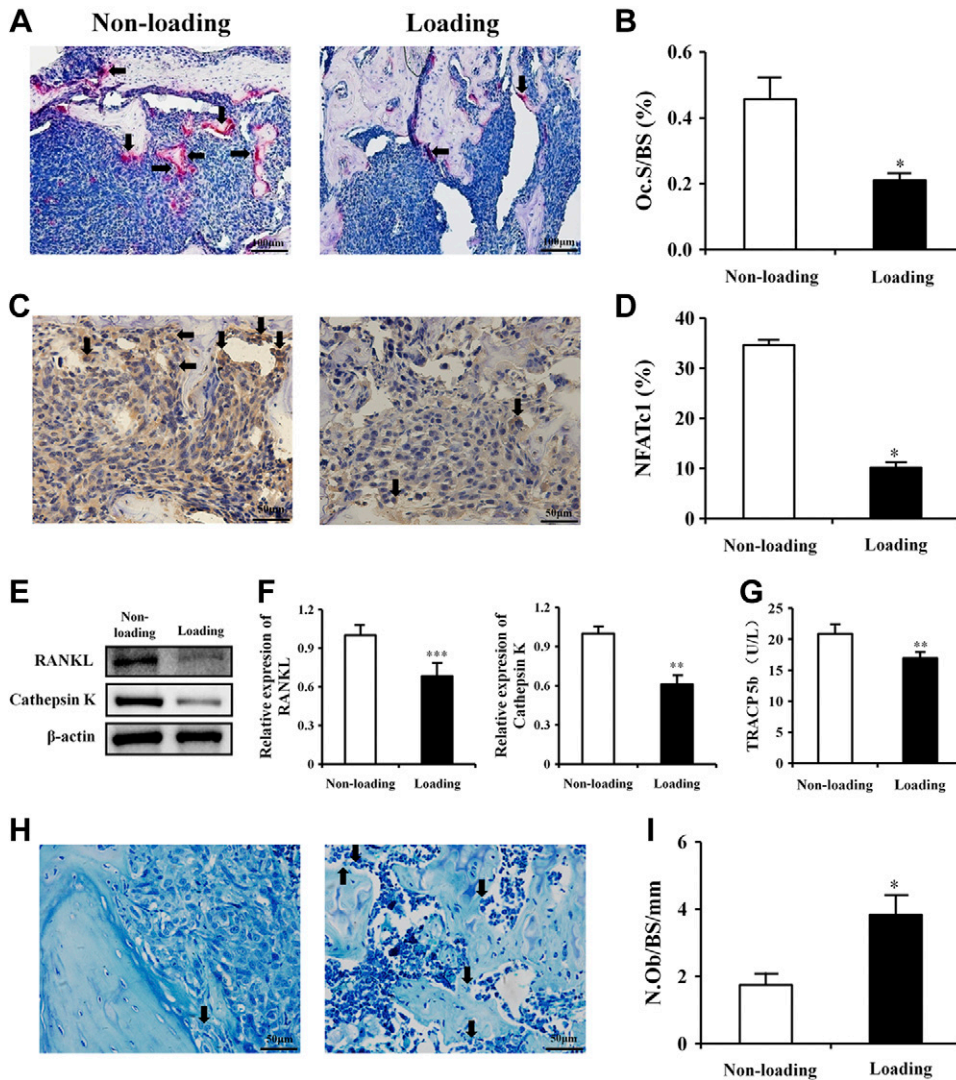
Figure 4. Effect of ankle loading on activities of osteoclasts and osteoblasts. *A*) TRAP staining for evaluation of bone resorption (original magnification, ×200; scale bar, 100 μm). Red staining shows TRAP-positive osteoclasts. The arrow indicates positive signal. *B*) TRAP staining showing an increase in the ratio of the number of TRAP-positive cells in the model group ($P < 0.05$). *C, D*) NFATc1 expression detected by immunohistochemistry ($P < 0.05$; original magnification, ×400; scale bar, 50 μm). The positive expression is indicated by the arrow ($n = 10$). *E, F*) Representative images of Western blotting (*E*) with ankle loading. The levels of RANKL and cathepsin K (*F*) are shown ($n = 5$) (all $P < 0.05$). *G*) Serum TRACP-5b analyses ($n = 5$). *H, I*) MacNeal's staining for identifying osteoblasts (*H*) (original magnification, ×400; scale bar, 50 μm). Osteoblasts, located on the trabecular surface, are indicated by the arrows. The number of osteoblasts was quantified (*I*) ($n = 10$) ($P < 0.05$). *$P < 0.05$.

significantly suppressed its loss. Compared with the loading group, tumor growth and associated bone loss were higher in the nonloading group. Ankle loading increased BV/TV, Tb.N, and Tb.Th as well as decreased the spacing of trabeculae. Ankle loading also elevated structural integrity of the tibia and improved cancellous bone microarchitecture. Histopathological examination showed that ankle loading reduced tumor area. Immunohistochemistry staining and Western blotting further validated the effects of ankle loading on suppression of tumor growth and bone resorption. Correlation analysis and multiple linear regression models showed a strong relationship between tumor burden and osteoclast/osteoblast activities. These findings support potential therapeutic effects of ankle loading on breast cancer–associated bone metastasis in tibia.

A variety of reports show that physical activity can reduce cancer-related morbidity and offers an important role in rehabilitation (37–39). The skeleton is sensitive to its mechanical environment, and physical stimulation contributes to maintaining bone mass. Other treatments, including radiation and administration of chemotherapeutic drugs (*i.e.*, bisphosphonates),

may often present strong side effects, which are, in certain cases, life-threatening (9). Unlike walking and jogging, which cannot be achieved by patients who are bed-laden, mechanical loading, such as ankle loading, may offer an alternative physical stimulation that is easily applied. In our previous studies, it is demonstrated that mechanical loading can reduce bone resorption by inhibiting development of osteoclasts and promoting osteoblastogenesis to enhance bone remodeling. *In vivo* experiments showed that mechanical loading reduces the number of osteoclasts, and molecular experiments revealed that the expression of osteoclast-related factors decreases after mechanical loading. *In vitro* analysis confirmed that mechanical loading inhibited differentiation, migration, and adhesion of osteoclasts (22, 23, 40). Our previous study showed that responsiveness to ankle loading differs in the periosteum and endosteum. In the endosteum, the proximal section near the knee is more responsive than other sections. The bone formation rate with ankle loading is highest in the proximal endosteum (19), and mechanical loading can inhibit inflammatory response–related factors, such as TNF-α, MMP13, and NF-κB
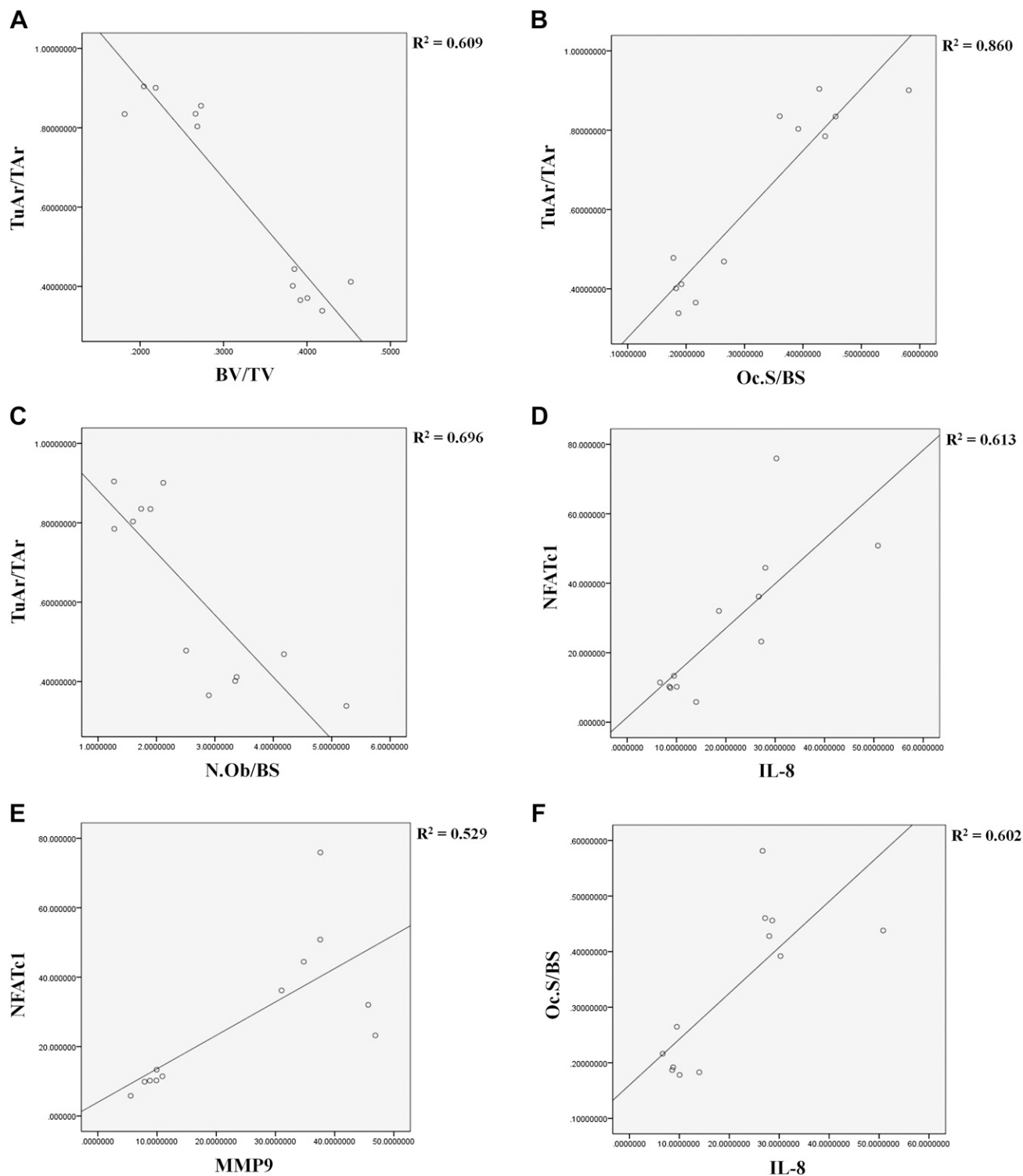
Figure 5. Correlation analysis. *A–E*) Correlations among BV/TV (*A*), osteoclast number (Oc.S/BS) (*B*), and osteoblast number (N.Ob/BS) (*C*) and TuAr/TAr. Correlations among IL-8 (*D*) and MMP9 (*E*) and NFATc1. *F*) Correlations between osteoclast number (Oc.S/BS) and IL-8 ($n = 6$).

(23). Mechanical loading induces periodic deformation in the epiphysis that drives alteration of intramedullary pressure in the medullary cavity and interstitial fluid flow in the lacunocanalicular network in the diaphysis (20, 21). Our experiments showed that ankle loading can not only reduce tumor growth but also restore bone microarchitecture in tibia. In the current preclinical study, ankle loading presented multiple beneficial effects by suppressing tumor growth and bone resorption, as well as promoting bone formation (**Fig. 6**).

We monitored body weight and body composition, in which mechanical loading alleviated a rapid decline in body weight and body composition. Cancer cachexia was reported to be associated with severe weight loss, a sign of
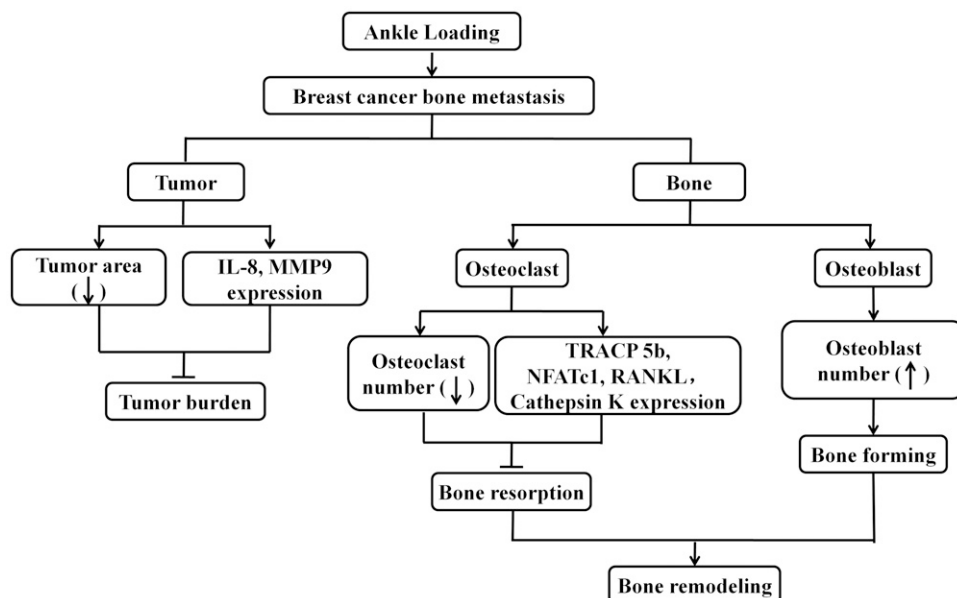
Figure 6. Proposed mechanism of ankle loading's action on breast cancer–associated bone metastasis.

impending death. Although robust evidence for interventions to manage unintentional weight loss in advanced cancer is needed, low weight apparently accelerates patient death (41, 42). Our observation is consistent with the notion that mechanical loading suppresses the rapid decline of body weight and body composition by inhibiting cachexia. H&E staining showed that ankle loading suppressed tumor growth in the tibia. Several reports showed that chemokine IL-8 was able to directly stimulate osteoclastogenesis, which played a critical role in breast cancer progression (43, 44). Among all MMP members, MMP9 was correlated with tumor metastasis. Inhibition of MMP9 undermines the capability of bone degradation by tumor metastasis (45, 46). The result herein clearly showed that ankle loading reduced expression of IL-8 and MMP9 and inhibited tumor growth and progression. TRAP staining suggested that the osteoclast number in the tibia with loading is significantly fewer than that in the nonloading group. Genes such as NFATc1, RANKL, and cathepsin K are important for osteoclast development (23, 47–49). The result of this study indicated that ankle loading suppressed activity of osteoclasts by regulating NFATc1, RANKL, cathepsin K. In addition, bone formation in the tibia was promoted by ankle loading with an increase in the number of osteoblasts. It is reported that ankle loading induces bone formation through TGF-β or Wnt signaling (19, 50). Because TGF-β and Wnt signaling are also involved in tumor growth and migration, further analysis is needed to evaluate the roles of these pathways in preventing bone loss and regulating tumor progression.

Our *in vivo* loading experiment presented several limitations. First, we used BALB/c mice and direct intratibial injection of 4T1 cells. Although a majority of breast cancer may metastasize to specific bones, such as the spine, pelvis, and ribs, few mouse models for metastases to those bones are available. Intratibia injection is popularly used (30–32), although intracardiac injection is employed to mimic invasion of tumor cells into the tibia. In this study, we chose intratibial injection because intracardiac injection presented a low rate of bone metastasis and a relatively high rate of mortality. Second, we focused on the selected genes and their loading-driven alteration. The role of each of those genes needs to be further analyzed with and without ankle loading.

In summary, we demonstrate in the mouse model that ankle loading is effective in protecting bone from breast cancer–associated metastasis. It can prevent tumor growth and bone degradation by simultaneously suppressing osteoclastogenesis and promoting osteogenesis. Further studies should be performed to clarify the molecular mechanism underlying the ankle loading action on bone protection. The present study suggests that mechanical loading like ankle loading might have an advantage for protecting bone without directly applying mechanical loads to the site of tumor-induced osteolysis. **FJ**

AUTHOR CONTRIBUTIONS

S. Yang, H. Liu, L. Zhu, X. Li, and X. Song conducted research; S. Yang, H. Liu, D. Liu, H. Yokota, and P. Zhang analyzed the data; S. Yang and P. Zhang wrote the manuscript, approved the final manuscript as submitted,

and designed the research; and P. Zhang accepted responsibility for the integrity of the data analysis.

REFERENCES

1. Stevens, R. G., Brainard, G. C., Blask, D. E., Lockley, S. W., and Motta, M. E. (2014) Breast cancer and circadian disruption from electric lighting in the modern world. *CA Cancer J. Clin.* **64**, 207–218

2. Hong, W., and Dong, E. (2014) The past, present and future of breast cancer research in China. *Cancer Lett.* **351**, 1–5

3. Coleman, R. E. (2006) Clinical features of metastatic bone disease and risk of skeletal morbidity. *Clin. Cancer Res.* **12**, 6243s–6249s

4. Kuchuk, I., Hutton, B., Moretto, P., Ng, T., Addison, C. L., and Clemons, M. (2013) Incidence, consequences and treatment of bone metastases in breast cancer patients-experience from a single cancer centre. *J. Bone Oncol.* **2**, 137–144

5. Zhang, H., Zhu, W., Biskup, E., Yang, W., Yang, Z., Wang, H., Qiu, X., Zhang, C., Hu, G., and Hu, G. (2018) Incidence, risk factors and prognostic characteristics of bone metastases and skeletal-related events (SREs) in breast cancer patients: a systematic review of the real world data. *J. Bone Oncol.* **11**, 38–50

6. Loibl, S., Denkert, C., and von Minckwitz, G. (2015) Neoadjuvant treatment of breast cancer–clinical and research perspective. *Breast* **24** (Suppl 2), S73–S77

7. Erdogan, B., and Cicin, I. (2014) Medical treatment of breast cancer bone metastasis: from bisphosphonates to targeted drugs. *Asian Pac. J. Cancer Prev.* **15**, 1503–1510

8. Lüftner, D., Niepel, D., and Steger, G. G. (2018) Therapeutic approaches for protecting bone health in patients with breast cancer. *Breast* **37**, 28–35

9. Rollason, V., Laverrière, A., MacDonald, L. C., Walsh, T., Tramèr, M. R., and Vogt-Ferrier, N. B. (2016) Interventions for treating bisphosphonate-related osteonecrosis of the jaw (BRONJ). *Cochrane Database Syst. Rev.* **2**, CD008455

10. Schneeweiss, A., Lux, M. P., Janni, W., Hartkopf, A. D., Nabieva, N., Taran, F. A., Overkamp, F., Kolberg, H. C., Hadji, P., Tesch, H., Wöckel, A., Ettl, J., Lüftner, D., Wallwiener, M., Müller, V., Beckmann, M. W., Belleville, E., Wallwiener, D., Brucker, S. Y., Schütz, F., Fasching, P. A., and Fehm, T. N. (2018) Update breast cancer 2018 (part 2) - advanced breast cancer, quality of life and prevention. *Geburtshilfe Frauenheilkd.* **78**, 246–259

11. Lahart, I. M., Metsios, G. S., Nevill, A. M., and Carmichael, A. R. (2015) Physical activity, risk of death and recurrence in breast cancer survivors: a systematic review and meta-analysis of epidemiological studies. *Acta Oncol.* **54**, 635–654

12. Zhong, S., Jiang, T., Ma, T., Zhang, X., Tang, J., Chen, W., Lv, M., and Zhao, J. (2014) Association between physical activity and mortality in breast cancer: a meta-analysis of cohort studies. *Eur. J. Epidemiol.* **29**, 391–404

13. Jones, L. W., and Alfano, C. M. (2013) Exercise-oncology research: past, present, and future. *Acta Oncol.* **52**, 195–215

14. Yee, J., Davis, G. M., Beith, J. M., Wilcken, N., Currow, D., Emery, J., Phillips, J., Martin, A., Hui, R., Harrison, M., Segelov, E., and Kilbreath, S. L. (2014) Physical activity and fitness in women with metastatic breast cancer. *J. Cancer Surviv.* **8**, 647–656

15. Pedersen, L., Idorn, M., Olofsson, G. H., Lauenborg, B., Nookaew, I., Hansen, R. H., Johannesen, H. H., Becker, J. C., Pedersen, K. S., Dethlefsen, C., Nielsen, J., Gehl, J., Pedersen, B. K., Thor Straten, P., and Hojman, P. (2016) Voluntary running suppresses tumor growth through epinephrine- and il-6-dependent nk cell mobilization and redistribution. *Cell Metab.* **23**, 554–562

16. Sheill, G., Guinan, E. M., Peat, N., and Hussey, J. (2018) Considerations for exercise prescription in patients with bone metastases: a comprehensive narrative review. *PM R* **10**, 843–864

17. Lynch, M. E., Brooks, D., Mohanan, S., Lee, M. J., Polamraju, P., Dent, K., Bonassar, L. J., van der Meulen, M. C., and Fischbach, C. (2013) In vivo tibial compression decreases osteolysis and tumor formation in a human metastatic breast cancer model. *J. Bone Miner. Res.* **28**, 2357–2367

18. Pagnotti, G. M., Chan, M. E., Adler, B. J., Shroyer, K. R., Rubin, J., Bain, S. D., and Rubin, C. T. (2016) Low intensity vibration mitigates tumor progression and protects bone quantity and quality in a murine model of myeloma. *Bone* **90**, 69–79

19. Zhang, P., Turner, C. H., and Yokota, H. (2009) Joint loading-driven bone formation and signaling pathways predicted from genome-wide expression profiles. *Bone* **44**, 989–998

20. Zhang, P., Malacinski, G. M., and Yokota, H. (2008) Joint loading modality: its application to bone formation and fracture healing. *Br. J. Sports Med.* **42**, 556–560

21. Zhang, P., Hamamura, K., Yokota, H., and Malacinski, G. M. (2009) Potential applications of pulsating joint loading in sports medicine. *Exerc. Sport Sci. Rev.* **37**, 52–56

22. Liu, D., Li, X., Li, J., Yang, J., Yokota, H., and Zhang, P. (2015) Knee loading protects against osteonecrosis of the femoral head by enhancing vessel remodeling and bone healing. *Bone* **81**, 620–631

23. Li, X., Yang, J., Liu, D., Li, J., Niu, K., Feng, S., Yokota, H., and Zhang, P. (2016) Knee loading inhibits osteoclast lineage in a mouse model of osteoarthritis. *Sci. Rep.* **6**, 24668

24. Kakhki, V. R. D., Anvari, K., Sadeghi, R., Mahmoudian, A. S., and Torabian-Kakhki, M. (2013) Pattern and distribution of bone metastases in common malignant tumors. *Nucl. Med. Rev. Cent. East. Eur.* **16**, 66–69

25. Wang, Q., Mo, J., Zhao, C., Huang, K., Feng, M., He, W., Wang, J., Chen, S., Xie, Z., Ma, J., and Fan, S. (2018) Raddeanin A suppresses breast cancer-associated osteolysis through inhibiting osteoclasts and breast cancer cells. *Cell Death Dis.* **9**, 376

26. Kamalakar, A., Bendre, M. S., Washam, C. L., Fowler, T. W., Carver, A., Dilley, J. D., Bracey, J. W., Akel, N. S., Margulies, A. G., Skinner, R. A., Swain, F. L., Hogue, W. R., Montgomery, C. O., Lahiji, P., Maher, J. J., Leitzel, K. E., Ali, S. M., Lipton, A., Nicholas, R. W., Gaddy, D., and Suva, L. J. (2014) Circulating interleukin-8 levels explain breast cancer osteolysis in mice and humans. *Bone* **61**, 176–185

27. Ell, B., and Kang, Y. (2012) SnapShot: bone metastasis. *Cell* **151**, 690–690.e1

28. Merdad, A., Karim, S., Schulten, H. J., Dallol, A., Buhmeida, A., Al-Thubaity, F., Gari, M. A., Chaudhary, A. G., Abuzenadah, A. M., and Al-Qahtani, M. H. (2014) Expression of matrix metalloproteinases (MMPs) in primary human breast cancer: MMP-9 as a potential biomarker for cancer invasion and metastasis. *Anticancer Res.* **34**, 1355–1366

29. Ma, Y. V., Lam, C., Dalmia, S., Gao, P., Young, J., Middleton, K., Liu, C., Xu, H., and You, L. (2018) Mechanical regulation of breast cancer migration and apoptosis via direct and indirect osteocyte signaling. *J. Cell. Biochem.* **119**, 5665–5675

30. Wright, L. E., Ottewell, P. D., Rucci, N., Peyruchaud, O., Pagnotti, G. M., Chiechi, A., Buijs, J. T., and Sterling, J. A. (2016) Murine models of breast cancer bone metastasis. *Bonekey Rep.* **5**, 804

31. Duong, L. T., Wesolowski, G. A., Leung, P., Oballa, R., and Pickarski, M. (2014) Efficacy of a cathepsin K inhibitor in a preclinical model for prevention and treatment of breast cancer bone metastasis. *Mol. Cancer Ther.* **13**, 2898–2909

32. Lee, J. H., Kim, B., Jin, W. J., Kim, J. W., Kim, H. H., Ha, H., and Lee, Z. H. (2014) Trolox inhibits osteolytic bone metastasis of breast cancer through both PGE2-dependent and independent mechanisms. *Biochem. Pharmacol.* **91**, 51–60

33. Taipaleenmäki, H., Browne, G., Akech, J., Zustin, J., van Wijnen, A. J., Stein, J. L., Hesse, E., Stein, G. S., and Lian, J. B. (2015) Targeting of runx2 by mir-135 and mir-203 impairs progression of breast cancer and metastatic bone disease. *Cancer Res.* **75**, 1433–1444

34. Zhang, W., Rhodes, S. D., Zhao, L., He, Y., Zhang, Y., Shen, Y., Yang, D., Wu, X., Li, X., Yang, X., Park, S. J., Chen, S., Turner, C., and Yang, F. C. (2011) Primary osteopathy of vertebrae in a neurofibromatosis type 1 murine model. *Bone* **48**, 1378–1387

35. Lumachi, F., Basso, S. M., Camozzi, V., Tozzoli, R., Spaziante, R., and Ermani, M. (2016) Bone turnover markers in women with early stage breast cancer who developed bone metastases. A prospective study with multivariate logistic regression analysis of accuracy. *Clin. Chim. Acta* **460**, 227–230

36. D'Oronzo, S., Brown, J., and Coleman, R. (2017) The role of biomarkers in the management of bone-homing malignancies. *J. Bone Oncol.* **9**, 1–9

37. Tsianakas, V., Harris, J., Ream, E., Van Hemelrijck, M., Purushotham, A., Mucci, L., Green, J. S., Fewster, J., and Armes, J. (2017) CanWalk: a feasibility study with embedded randomised controlled trial pilot of a

walking intervention for people with recurrent or metastatic cancer. *BMJ Open* **7**, e013719

38. Ashcraft, K. A., Peace, R. M., Betof, A. S., Dewhirst, M. W., and Jones, L. W. (2016) Efficacy and mechanisms of aerobic exercise on cancer initiation, progression, and metastasis: a critical systematic review of in vivo preclinical data. *Cancer Res.* **76**, 4032–4050

39. Kim, J., Choi, W. J., and Jeong, S. H. (2013) The effects of physical activity on breast cancer survivors after diagnosis. *J. Cancer Prev.* **18**, 193–200

40. Li, X., Liu, D., Li, J., Yang, S., Xu, J., Yokota, H., and Zhang, P. (2019) Wnt3a involved in the mechanical loading on improvement of bone remodeling and angiogenesis in a postmenopausal osteoporosis mouse model. *FASEB J.* fj201802711R

41. Payne, C., Wiffen, P. J., and Martin, S. (2012) Interventions for fatigue and weight loss in adults with advanced progressive illness. *Cochrane Database Syst. Rev.* **1**, CD008427

42. Vagnildhaug, O. M., Blum, D., Wilcock, A., Fayers, P., Strasser, F., Baracos, V. E., Hjermstad, M. J., Kaasa, S., Laird, B., and Solheim, T. S.; European Palliative Care Cancer Symptom study group. (2017) The applicability of a weight loss grading system in cancer cachexia: a longitudinal analysis. *J. Cachexia Sarcopenia Muscle* **8**, 789–797

43. Selvaduray, K. R., Radhakrishnan, A. K., Kutty, M. K., and Nesaretnam, K. (2012) Palm tocotrienols decrease levels of pro-angiogenic markers in human umbilical vein endothelial cells (HUVEC) and murine mammary cancer cells. *Genes Nutr.* **7**, 53–61

44. Bendre, M. S., Montague, D. C., Peery, T., Akel, N. S., Gaddy, D., and Suva, L. J. (2003) Interleukin-8 stimulation of osteoclastogenesis and bone resorption is a mechanism for the increased osteolysis of metastatic bone disease. *Bone* **33**, 28–37

45. Wani, N., Nasser, M. W., Ahirwar, D. K., Zhao, H., Miao, Z., Shilo, K., and Ganju, R. K. (2014) C-X-C motif chemokine 12/C-X-C chemokine receptor type 7 signaling regulates breast cancer growth and metastasis by modulating the tumor microenvironment. *Breast Cancer Res.* **16**, R54

46. Luo, K. W., Yue, G. G., Ko, C. H., Gao, S., Lee, J. K., Li, G., Fung, K. P., Leung, P. C., and Lau, C. B. (2015) The combined use of Camellia sinensis and metronomic zoledronate in 4T1 mouse carcinoma against tumor growth and metastasis. *Oncol. Rep.* **34**, 477–487

47. Kim, J. H., and Kim, N. (2014) Regulation of nfatc1 in osteoclast differentiation. *J. Bone Metab.* **21**, 233–241

48. Kim, J. Y., Cheon, Y. H., Yoon, K. H., Lee, M. S., and Oh, J. (2014) Parthenolide inhibits osteoclast differentiation and bone resorbing activity by down-regulation of NFATc1 induction and c-Fos stability, during RANKL-mediated osteoclastogenesis. *BMB Rep.* **47**, 451–456

49. Lorenzo, J. (2017) The many ways of osteoclast activation. *J. Clin. Invest.* **127**, 2530–2532

50. Buenrostro, D., Kwakwa, K. A., Putnam, N. E., Merkel, A. R., Johnson, J. R., Cassat, J. E., and Sterling, J. A. (2018) Early TGF-β inhibition in mice reduces the incidence of breast cancer induced bone disease in a myeloid dependent manner. *Bone* **113**, 77–88